Mapping out emerging network structures in dynamic network models coupled with epidemics

István Z. Kiss, Luc Berthouze, Joel C. Miller and Péter L. Simon

Abstract We consider the susceptible - infected - susceptible (SIS) epidemic on a dynamic network model with addition and deletion of links depending on node status. We analyse the resulting pairwise model using classical bifurcation theory to map out the spectrum of all possible epidemic behaviours. However, the major focus of the chapter is on the evolution and possible equilibria of the resulting networks. Whereas most studies are driven by determining system-level outcomes, e.g., whether the epidemic dies out or becomes endemic, with little regard for the emerging network structure, here, we want to buck this trend by augmenting the system-level results with mapping out of the structure and properties of the resulting networks. We find that depending on parameter values the network can become disconnected and show bistable-like behaviour whereas the endemic steady state sees the emergence of networks with qualitatively different degree distributions. In particular, we observe de-phased oscillations of both prevalence and network degree during which there is role reversal between the level and nature of the connectivity of susceptible and infected nodes. We conclude with an attempt at describing what a potential bifurcation theory for networks would look like.

István Z. Kiss
Department of Mathematics, School of Mathematical and Physical Sciences, University of Sussex, Falmer, Brighton BN1 9QH, UK, e-mail: i.z.kiss@sussex.ac.uk

Luc Berthouze
Centre for Computational Neuroscience and Robotics, University of Sussex, Falmer, Brighton, BN1 9QH, UK e-mail: l.berthouze@sussex.ac.uk

Joel C. Miller
School of Mathematical Sciences and School of Biological Sciences, Monash University, Clayton, VIC Australia, Monash Academy for Cross and Interdisciplinary Mathematics, and Institute for Disease Modeling, Bellevue, WA USA e-mail: joel.c.miller@gmail.com

Péter L. Simon
Institute of Mathematics, Eötvös Loránd University Budapest, and Numerical Analysis, and Large Networks Research Group, Hungarian Academy of Sciences, Hungarye-mail: simonp@cs.elte.hu

1 Introduction

Networks have been and remain extremely useful in modelling complex systems. Their use has led to rapid progress in the study of stochastic spreading processes such as information, rumour and epidemics. The role of contact heterogeneity, preferential mixing and (to a lesser extent) of clustering is now well understood [3, 17, 11]. Mean-field models ranging from heterogenous mean-field [17], pairwise [10, 5, 9] and effective-degree [13, 1] to edge-based compartmental models [16, 15] have proved crucial in circumventing the technical analysis of the underlying stochastic process. This shifts the focus onto the analysis of low-dimensional systems of ordinary differential equations, where variables are system-level expected values such as the the number of nodes and edges of different statuses.

Attempting to account for more realistic features of spreading processes (e.g., non-exponentially-distributed waiting times) or networks (e.g., clustered and/or with higher-order structure, time-varying or embedded in some space) leads to models that are more complex, harder to analyse and less transparent. Indeed, this typically requires (i) more complex network models, including a better understanding of the properties of empirical networks, or (ii) the derivation of new or refined mean-field models which may require sophisticated mathematical tools or techniques.

In this chapter we focus on the latter and consider a model where the epidemic dynamics on the network is coupled with a network which evolves in time. Several studies have already made important observations regarding how coupling the dynamics on the network with that of the network may change or enrich the outcome of the epidemic. For example, [7] showed that for a rewiring process that preserved the number of links ("link number-preserving") where susceptible nodes cut links to infected nodes and instantaneously reconnect to a random susceptible node, can lead to oscillations, albeit over a very narrow area of the parameter space [8]. This model was later refined and extended either by considering a different rewiring mechanism (e.g., non link-preserving rewiring but still dependent on link status [22, 24, 25, 19]) or by modelling the same process but with more sophisticated models such as the effective degree [14]. For reviews on this topic, we refer the reader to [6, 20].

Such dynamic or adaptive networks present several challenges in that usually the resulting mean-field models are of a higher dimension than the static network equivalent. In many cases, this is explained by the fact that closures now involve dynamic or time-varying quantities (e.g., the average degree of the network) that need to be tracked via their own equations. But perhaps more important is the fact such coupled dynamics lead to correlations that usually violate the assumptions behind even the more complex closures. Still, mean-field models have an important role to play in providing a qualitative picture of the different behaviours of the system, and to guide a more rigorous analysis.

Despite ongoing progress in model refinement and accounting for more realistic scenarios of dynamic contact structures, very few studies focus on understanding and mapping out the structure of the emerging networks. While there is detailed information about when an epidemic dies out, there is value in knowing whether the epidemic died out due to the network being poorly connected or due to an un-

favourable ratio of infection to recovery rates despite the network being well connected. Other important insights may come from knowing whether the fluctuations in prevelance can lead to fluctuation in average degree of the network, whether the network can fall apart into disjointed components isolating the infection; or, finally, what the degree distribution will be at the endemic equilibrium or during oscillations in prevalence. In this chapter we set out to map out the structure of the emerging networks for an SIS epidemic coupled with a link status-dependent link addition and deletion model, where existing links are deleted and new links are created depending on the disease status of the nodes that these links connect.

The chapter is structured as follows. After formulating the model in Section 2, we provide a bifurcation analysis of the simple pairwise model describing the coupled epidemic and dynamic network model in Section 3. Section 4 is dedicated to mapping out the emerging network structure by using the compact pairwise model which tracks the degree of the nodes and by relying on explicit stochastic network simulations. We conclude with a discussion of our results identifying open questions and new directions for further research.

2 Model formulation

This chapter considers *SIS* (susceptible-infected-susceptible) epidemic propagation on an adaptive network with link status-dependent link activation and deletion. Specifically, the model incorporates the following independent Poisson processes:

- **Infection:** Infection is transmitted across each contact between an I and an S node, or $(I-S)$ link, at rate τ,
- **Recovery:** Each I node recovers (becoming an S node) at rate γ independently of the network,
- **Link activation:** A non-existing link between a node of status A and another of status B is activated at rate α_{AB}, with $A,B \in \{S,I\}$,
- **Link deletion:** An existing link between a node of status A and another of status B is terminated at rate ω_{AB}, with $A,B \in \{S,I\}$.

This model is significantly different from 'smart' rewiring [6], where S nodes have full knowledge of the status of all other nodes and choose to minimise their exposure to infection by cutting links to I neighbours and immediately rewiring to a randomly chosen S node. This latter approach conserves the number of links in the network and simplifies the analysis of the resulting system, by not having to consider an evolving average degree.

Here, we set out to explore and explain the spectrum of system behaviours with special focus on understanding and mapping the evolution of the network structure and attainable network equilibria. The first task is carried out via classical bifurcation analysis at system level and focuses on identifying regimes such as die-out, endemic equilibria and oscillations.

In order to do this, we will employ a number of approaches including: (i) two different types of pairwise or pair-based mean-field ODE models, and (ii) full network-based stochastic simulation. Regarding the rewiring parameters we focus on two scenarios, namely:

A. $\alpha_{SI} = \alpha_{II} = \alpha_{SS} = \alpha$ and $\omega_{SI} = \omega_{II} = \omega_{SS} = \omega$, and
B. $\alpha_{SI} = \alpha_{II} = 0$ and $\alpha_{SS} \neq 0$, and $\omega_{II} = \omega_{SS} = 0$ and $\omega_{SI} \neq 0$.

While the first is link status-independent and leads to simpler and more tractable models, the second is motivated by practical considerations, such as those used in the 'smart' rewiring – where nodes aim to minimise the risk of becoming infected while maintaining their connectivity to the network.

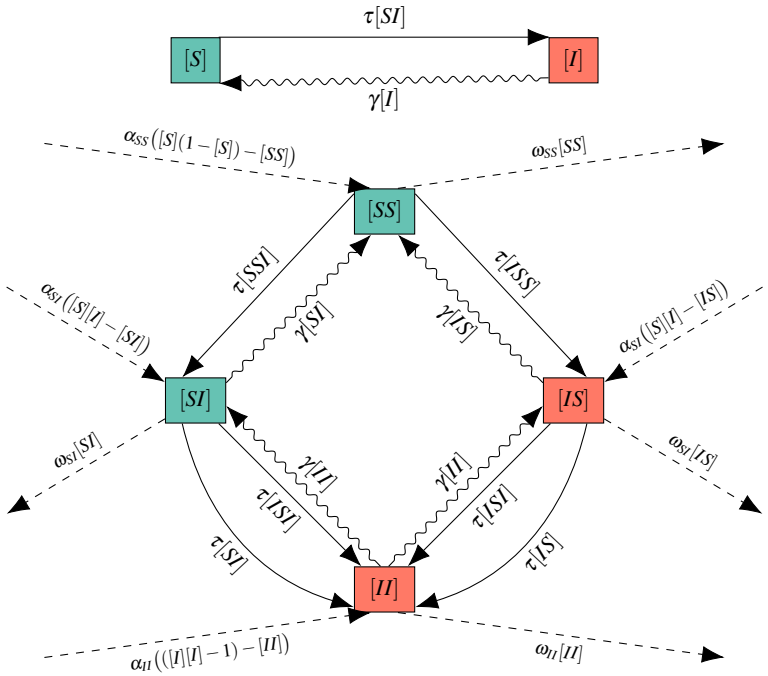

Fig. 1: A flow diagram leading to system (1). (top) The relevant flows for the individual-level variables. The solid line denotes an infection, while the sinuous line denotes a recovery. The rate of new infecteds depends on $[SI]$, and so we require pair-level variables. (bottom) The relevant flows for the pair-level variables. The colours denote the status of the "first" node in the edge. The solid lines denote infections, the sinuous lines denote recoveries, and the dashed lines denote addition or removal of edges. Some of the infection events involve triples, and so we need triple-level variables or a closure.

We start by formulating the pairwise model for the expected number of nodes and pairs of different statuses. As was shown in [12], this gives rise to

$$[\dot{I}] = \tau[SI] - \gamma[I], \tag{1a}$$

$$[\dot{SI}] = \gamma([II] - [SI]) + \tau([SSI] - [ISI] - [SI]) + \alpha_{SI}\big([S][I] - [SI]\big) - \omega_{SI}[SI], \tag{1b}$$

$$[\dot{II}] = -2\gamma[II] + 2\tau([ISI] + [SI]) + \alpha_{II}\big([I]([I] - 1) - [II]\big) - \omega_{II}[II], \tag{1c}$$

$$[\dot{SS}] = 2\gamma[SI] - 2\tau[SSI] + \alpha_{SS}\big([S]([S] - 1) - [SS]\big) - \omega_{SS}[SS]. \tag{1d}$$

These equations can be interpreted using Fig. 1. The basic idea of pairwise models is to derive evolution equations for the expected number of nodes of different statuses, i.e., $[X]$ where $X \in \{S, I\}$. However, looking at the evolution equation of $[I]$, see equation (1a), we note that this depends on the expected number of $[SI]$ pairs, and hence equations for this and other pairs, e.g., $[SS]$ and $[II]$, are also needed. The evolution equations of pairs will then depend on the expected number of triples with nodes of certain statuses, i.e., $[SSI]$ and $[ISI]$. This leads to a hierarchical dependence of pairs on triples and then of triples on quadruples, and so on. This is obviously not practical due to the combinatorial explosion in number of equations. Hence, a closure is needed which in this case approximates triples in terms of singles and pairs. From the model it follows that $[S] + [I] = N$, and that the closure requires the time-dependent expected average degree of S nodes. This is given by

$$k_S(t) = \frac{[SS] + [SI]}{[S]}. \tag{2}$$

The well-known closure [10] is used, namely

$$[SSI] = \frac{(k_S - 1)[SS][SI]}{k_S[S]} \text{ and } [ISI] = \frac{(k_S - 1)[SI][SI]}{k_S[S]}. \tag{3}$$

Upon applying these closures, a self-consistent system with 4 ODEs is obtained. This can be analysed using classical bifurcation theory techniques.

It is worth noting that the pairwise model above makes some implicit assumptions. First, it assumes that pairs and triples are counted multiple times. This for example implies that $[SI] = [IS]$ and that $[SS]$ stands for twice the number of singly counted edges connecting susceptible nodes. Similarly, $[ISI]$ is a multiple count of arrangements such as nodes i, j and k, with susceptible node j being connected to infected nodes i and k. Second, our model does not explicitly account for the degree of nodes and thus degree-degree correlations are omitted. Finally, we note that closures use the time-dependent excess degree of susceptible nodes, $k_S(t)$, rather than the average degree of the network, $\langle k \rangle$, as it is done for static network models.

3 Bifurcation analysis of the epidemic

3.1 Bifurcation analysis of the system behaviour for scenario A

Turning to scenario **A**, i.e., the case in which edges are added or removed independently of node status ($\alpha_{SS} = \alpha_{SI} = \alpha_{II} := \alpha$ and $\omega_{SS} = \omega_{SI} = \omega_{II} := \omega$), we determine the steady states and the local behaviour around them. In [12] it was shown that the network becomes an Erdős-Rényi type random graph at the steady state and the probability an edge is active is $p = \frac{\alpha}{\alpha+\omega}$. So the average degree at equilibrium is

$$\langle k \rangle = (N-1)\frac{\alpha}{\alpha+\omega}$$

In this case the coordinates of the disease-free steady state are $[I] = 0$, $[SI] = 0$, $[II] = 0$ and $[SS] = \frac{N(N-1)\alpha}{\omega+\alpha}$. The Jacobian matrix corresponding to this steady state is

$$J = \begin{pmatrix} -\gamma & \tau & 0 & 0 \\ \alpha N & \tau(\langle k \rangle - 2) - \alpha - \gamma - \omega & \gamma & 0 \\ -\alpha & 2\tau & -2\gamma - \alpha - \omega & 0 \\ \alpha(-2N+1) & 2\gamma - 2\tau(\langle k \rangle - 1) & 0 & -\alpha - \omega \end{pmatrix},$$

Solving the equation $\det J = 0$ for τ shows that a transcritical bifurcation occurs at

$$\tau_c = \frac{\gamma(2\gamma + \alpha + \omega)}{\alpha N + 2\gamma(\langle k \rangle - 1)}, \tag{4}$$

which is derived in [23]. Numerical investigation shows that for $\tau < \tau_c$ the solutions of the system tend to the disease-free steady state, while for $\tau > \tau_c$ the solutions converge to the endemic steady state. Oscillations were not observed in this case, see [23].

An approximation to this bifurcation curve can be determined by theoretical considerations. The simplest way of approximating the transcritical bifurcation curve, which separates the endemic and disease-free regions, is to start from the steady state equation $\tau[SI] = \gamma[I]$ and make an additional assumption (the pair closure) $[SI] \approx \frac{\langle k \rangle}{N-1}[S][I]$. Substituting this into the steady state equation with $\langle k \rangle = N\alpha/(\alpha+\omega)$, then dividing by $[I]$ and substituting $[S] = N$, which holds at the boundary of the endemic region, we arrive at

$$\tau_{pc} = \gamma\frac{\alpha+\omega}{N\alpha},$$

where the subscript 'pc' denotes pairwise closure. This bifurcation curve and that given by the pairwise model, see (4), are shown in Fig. 2. As expected the agreement is only partial since the pairwise model provides a more accurate approximation of the true stochastic model.

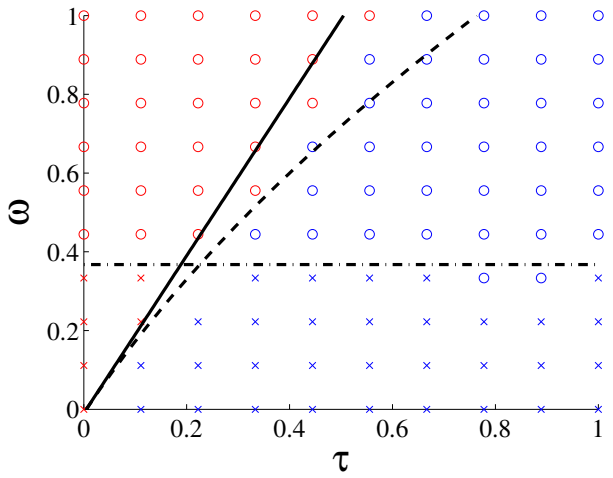

Fig. 2: Four behaviours observed in simulations of scenario **A** in the (τ, ω) parameter space and the theoretical bifurcation curves for $\alpha = 0.01$, $N = 200$, $\gamma = 1$. The horizontal line (dash-dotted line) represents the boundary of the parameter domain where the graph transitions from connected to disconnected. In the simulation, networks which on average had at least 3 disjointed components were considered disconnected. The other two curves are the transcritical bifurcation curves obtained from the mean-field approximation (continuous diagonal line) and from the pairwise approximation (4) (dashed line). The markers are as follows: $\times$ - connected, epidemic, $\times$ - connected, no epidemic, $\circ$ - disconnected, epidemic, and $\circ$ - disconnected, no epidemic.

3.2 Bifurcation analysis of the system behaviour for scenario B

Focusing on scenario **B**, the system admits two equilibria: (a) a disease-free equilibrium $([S],[I],[SI],[II],[SS]) = (N,0,0,0,N(N-1))$ and (ii) an endemic equilibrium which emerges from the solution of a quartic equation.

The linearisation around the disease-free steady state gives rise to a 4×4 Jacobian, the eigenvalues of which can be determined explicitly, see Appendix A in [24]. As shown, two of the eigenvalues are always negative and the remaining two have negative real part if and only if

$$\omega_{SI} > \tau(N-2) - \gamma, \tag{5}$$

which gives rise to a transcritical bifurcation where $\omega_{SI} = \tau(N-2) - \gamma$, see Fig. 3. Thus the following Proposition holds.

Proposition 1 *The disease-free steady state is stable if and only if* $\omega_{SI} > \tau(N-2) - \gamma$.

As mentioned above the endemic steady state is the solution of a quartic equation, see [24] for its detailed derivation. The analysis of this equation leads to the following proposition concerning the existence of the endemic steady state.

Proposition 2 *If $[S] = x \in (0,N)$ is a root of polynomial*

$$x^4 + A_3 x^3 + A_2 x^2 + A_1 x + A_0 = 0, \tag{6}$$

with

$$\begin{aligned}
A_3 &= 4ab - 3 - 2b - c,\\
A_2 &= 2 + 2b + c + b^2 + bc - 6ab - 4ab^2 - 2abc + 4a^2b^2 + Nb(1-4a),\\
A_1 &= Nb(-1 + 6a - b - c + 6ab + 2ac - 8a^2b),\\
A_0 &= 2N^2ab^2(1-2a),
\end{aligned}$$

where $a = \frac{\omega_{SI}}{\alpha_{SS}}$, $b = \frac{\gamma}{\tau}$ and $c = \frac{\omega_{SI}}{\tau}$, then the system has an endemic steady state, the coordinates of which can be given as

$$[S]_{ss} = x, \quad [I]_{ss} = N - x, \quad [SI]_{ss} = \frac{\gamma}{\tau}(N-x),$$

$$[SS]_{ss} = x(x-1) - 2\frac{\omega_{SI}\gamma}{\alpha_{SS}\tau}(N-x), \quad [II]_{ss} = \frac{\gamma(N-x)^2}{\tau x} + \frac{(N-x)[SS]_{ss}}{[SS]_{ss} + [SI]_{ss}}.$$

Extensive numerical tests suggest that the quartic polynomial has a single root providing a biologically plausible steady state. This means that below the transcritical bifurcation there is a unique endemic steady state. That is for a fixed value of τ, there is a critical cutting rate ω_{SI}^{crit} such that the unique endemic steady state exists if and only if $\omega_{SI} < \omega_{SI}^{crit} = \tau(N-2) - \gamma$.

Similarly, the stability of the endemic steady state can only be computed numerically by evaluating the coefficients of the characteristic polynomial. However, this does not prevent us from mapping out where the Hopf bifurcation arises (see Appendix A in [24] for details). It has been shown that the Hopf bifurcation points carve out an island from the parameter space, as shown in Fig. 3, within which the prevalence exhibits stable oscillations. Hence, the region below the transcritical bifurcation line and outside the Hopf island is where the endemic equilibrium is stable. It is important to note that the system-level analysis can be complemented by the observation that the expected average degree displays a behaviour similar to that of the expected number of infected nodes, as illustrated by the top panel of Fig. 6 but produced using the compact pairwise model.

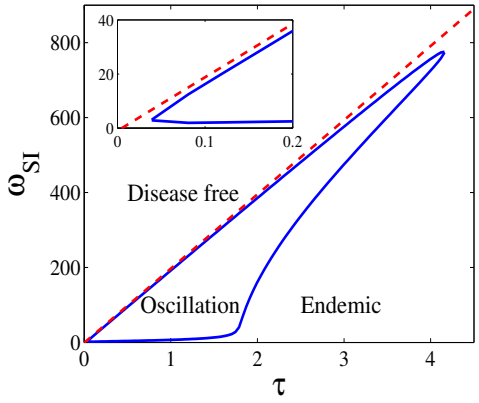

Fig. 3: Bifurcation diagram for the pairwise ODE model for scenario **B** in the (τ, ω_{SI}) parameter space for $N = 200$, $\gamma = 1$ and $\alpha_{SS} = 0.04$. The transcritical bifurcation occurs along the dashed line, and the Hopf bifurcation occurs along the perimeter of the island.

4 Network bifurcation

While some studies of adaptive or dynamic networks do consider and analyse changes in network structure [7, 14, 25], there are many papers which only focus on disease-related quantities such as the prevalence of infection with the aim to characterise those via bifurcation analysis.

However, it has been observed that the networks themselves can also undergo significant changes in time depending on parameters. For example, Gross et al. [7] reported segregation of networks into different components, see Fig. 7 also. Such analysis can reveal important network features which can invalidate the use of mean-field or pairwise models and, more importantly, may reveal the true impact of the interplay between dynamics on and of the network on changes in the underlying networks and the range of emerging networks.

Emergence of network structure from such dynamic network models could also be interpreted as a more natural or organic form of emergence of structure, compared to that observed in artificial or synthetic network models. In what follows we aim to couple the analysis of system- and network-level changes, in order to concurrently reveal the spectrum of behaviours at all levels, i.e., both system and network.

4.1 Mapping the emerging network structure onto the system-level bifurcation picture for scenario A

In the case of scenario **A**, that is, when $\alpha_{SI} = \alpha_{II} = \alpha_{SS} := \alpha$, and $\omega_{II} = \omega_{SS} = \omega_{SI} := \omega$ a more complete characterisation of network bifurcations can be achieved. As suggested by the pairwise model, two behaviours may occur according to the long time prevalence level, namely disease-free or endemic steady state. As regards the network structure we studied the connectivity (through determining the type and number of connected components) of the network and its degree distribution. Our goal here is to map out system and network behaviour over the (τ, ω) parameter space. We consider several stochastic simulations at each lattice point in the (τ, ω) parameter plane. The average epidemic level and network connectivity are then determined at the steady state (after a sufficiently long time). The different system and network level outcomes yield four different behaviours shown in Fig 2. The most interesting observation is that epidemics can be curtailed either because the network gets disconnected or because the epidemic is sub-threshold even though the network could theoretically support an epidemic.

The bifurcation curve separating the connected and disconnected regions can be derived analytically as follows. We have noted that at the steady-state this network is an Erdős–Rényi graph, with $p = \frac{\alpha}{\alpha+\omega}$, and we know that the threshold for an Erdős-Rényi graph being disconnected is $p = \frac{\ln N}{N}$ [2, 4], where N denotes the number of nodes. Taking into account these two formulas we get the following equation,

$$p = \frac{\alpha}{\alpha+\omega} = \frac{\ln N}{N}.$$

Thus the critical threshold for connectivity is,

$$\omega^* = \alpha\left(\frac{N}{\ln N} - 1\right). \tag{7}$$

The horizontal line in Fig. 2 is drawn at this value of ω, see also [23]. There is good agreement with the connectivity results obtained from simulation. Moreover, as expected, the degree distribution of networks during and at the end of simulations is well described by the binomial distribution and for fixed values of α, the number of components increases sharply with larger values of ω. This is quite natural since a higher cutting rate reduces the capacity of the epidemic to spread and thus the number of infected nodes. However, this leaves many susceptible nodes which will become more densely connected due to the addition of new $S-S$ links.

From system (1) and using scenario A it also follows that the number of (doubly-counted) edges in the network, $E(t) = [SS](t) + [II](t) + 2[SI](t)$, satisfies

$$\dot{E} = \alpha(N(N-1) - E) - \omega E \tag{8}$$

with its steady state being given by

$$E_{eq} = \frac{\alpha N(N-1)}{\alpha + \omega} \tag{9}$$

and with the average degree at equilibrium being $k_{eq} = \frac{E}{N} = \frac{\alpha(N-1)}{\alpha+\omega}$. This also follows from the simple heuristic argument that at equilibrium the rate at which edges are cut is equal to the rate at which edges are created, i.e., $\omega E_{eq} = \alpha(N(N-1) - E_{eq})$.

4.2 Mapping the emerging network structure onto the system-level bifurcation picture for scenario B

We now consider the more realistic case of a link status-dependent link addition and deletion model. While the system-level characterisation (i.e. focusing on the analysis of the pairwise model from the viewpoint of the outcome of the epidemic, without explicitly considering the underlying dynamic network) is not trivial, one can use classical bifurcation theory techniques even if some calculations can only be performed numerically. In [24] it was shown that the agreement between the pairwise model and simulation is mainly qualitative, insofar as the pairwise model predicts the observed outcomes but the size and boundaries of the different regimes in the parameter space differ between pairwise and simulation-based models. This is the result of the sub-optimal performance of closures which fail to capture the heterogeneity in degree distribution as well as, and perhaps more importantly, the presence of correlations introduced by the link status-dependent creation and deletion. These factors lead to the breakdown of closures. In addition, we shall show that the underlying network can become disconnected which further degrades the performance of the closures.

A detailed analysis of emerging network structures is made even more challenging by the need to rely on (i) different variants of pairwise models (tracking versus not tracking the degree of nodes), and (ii) explicit stochastic network-based simulation, sometimes on small networks to gain intuition. The former is useful to provide a rough guide of the possible behaviours and to identify broad parameter regions leading to networks of different type, such as connected versus disconnected, degree distributions that change throughout the oscillation cycle.

Analysing emerging networks using mean-field models

Let us progressively move from the simplest towards the most complex mean-field model and explore what information we can gain about the structure of the emerging networks. Starting with the pairwise model (1) one can ascertain at least the behaviour of the average degree over time. Thus, we can explore whether the average degree will stabilise or oscillate, and determine how these two regimes will

partition the parameter space considered in the bifurcation diagram at system-level shown in Fig. 3.

In Fig. 4 we show a contour plot of the average degree and we track the amplitude of oscillations of the average degree along an isoline where the mean average degree over an oscillatory cycle is constant. This figure reveals that the resulting networks exhibit a wide range of average degree values. Two important observations can be made. First, we note that for a fixed value of τ and as the cutting rate increases, the average degree at equilibrium (or its mean over one cycle) tends to higher values. This is due to the cutting of $S-I$ links which reduces the impact of the epidemic and leads to fewer infected nodes. This in turn leads to more susceptible nodes such that the addition of new $S-S$ links is fast and increases the average degree. Second, we note regions in which a form of bistability exists (see inset in the left panel of Fig. 4). Namely, the same average degree can be achieved for the same value of the transmission rate τ but two distinct values of ω_{SI}. This can be explained by considering the prevalence level (not shown) which, as intuition suggests, will be lower for higher values of the cutting rate and much higher for smaller values of ω_{SI}. Thus, networks with the same average degree and transmission rate can sustain either higher prevalence with a lower cutting rate or lower prevalence with a higher cutting rate.

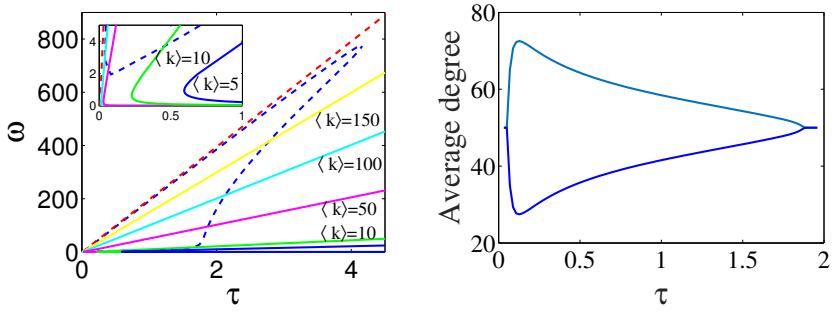

Fig. 4: (Left-panel) Contour plot of the average degree (or mean average degree over one cycle of oscillation when oscillations are stable) overlaid on the system-level bifurcation diagram. The inset provides a zoomed-in version of the bottom-left corner of the main plot to reveal the fine structure at low ω and τ values. (Right-panel) The amplitude of the oscillations of the average degree when travelling through the Hopf island along the isoline where the mean average degree is $\langle k\rangle = 50$. Parameter values are $N = 200$, $\gamma = 1$, $\alpha_{SS} = 0.04$.

The amplitude of the oscillations of the average degree in Fig. 4 confirms our expectations by showing that the amplitude tends to zero at the boundaries of the Hopf island and grows considerably when moving away from the boundary separating the stable endemic equilibrium and the oscillatory regime.

It is obvious that the previous model offers no information about how links are distributed over nodes, and thus about the degree distribution. To improve on this and get a basic description of the behaviour of the degree distribution one can write down a more complete set of pairwise equations that track the degree of nodes. Epidemics on networks with heterogeneous degrees can be described by heterogeneous mean-field models [5]. However, the number of equations in such models is of order $O(N^2)$ since the degree in a dynamic network can, in principle, vary between 0 and $N-1$, where N is the number of nodes in the network. As a trade-off between keeping degree heterogeneity and having a tractable system of ODEs, so-called compact pairwise models have been introduced [9]. The variables of this model are $[S_k]$ and $[I_k]$ representing the average number of susceptible and infected nodes of degree k, respectively, and the average number of pairs $[SI]$, $[SS]$ and $[II]$. We make use of the approximation

$$[A_kB] = [AB]\frac{k[A_k]}{\sum j[A_j]}, \tag{10}$$

where $[A_kB] = \sum_j [A_kB_j]$. In fact, the pairs $[A_kB_j]$ are not needed in the compact pairwise model, and only pairs of the form $[A_kB]$ are used, significantly reducing the number of equations. We extend this model with terms accounting for link addition/creation and deletion as follows. The deletion of links connecting an infected to a susceptible node with degree k at rate ω_{SI} contributes positively to $[S_{k-1}]$ and negatively to $[S_k]$. The creation of links connecting a susceptible to another susceptible node with degree k contributes negatively to $[S_k]$ with rate $\alpha_{SS}([S_k]([S]-1)-[S_kS])$ because the total number of such possible links is $[S_k]([S]-1)$ and the number of existing links is $[S_kS]$. The same process contributes positively to $[S_{k+1}]$. Using similar arguments we arrive at the following system,

$$\begin{aligned}
[\dot{S_k}] &= -\tau[S_kI] + \gamma[I_k] + \omega_{SI}([S_{k+1}I] - [S_kI]) && \text{(11a)}\\
&\quad + \alpha_{SS}\big([S_{k-1}]([S]-1) - [S_{k-1}S]\big) - \alpha_{SS}\big([S_k]([S]-1) - [S_kS]\big),\\
[\dot{I_k}] &= \tau[S_kI] - \gamma[I_k] + \omega_{SI}([I_{k+1}S] - [I_kS]), && \text{(11b)}\\
[\dot{SI}] &= \gamma([II] - [SI]) + \tau([SSI] - [ISI] - [SI]) - \omega_{SI}[SI], && \text{(11c)}\\
[\dot{II}] &= -2\gamma[II] + 2\tau([ISI] + [SI]), && \text{(11d)}\\
[\dot{SS}] &= 2\gamma[SI] - 2\tau[SSI] + \alpha_{SS}\big([S]([S]-1) - [SS]\big), && \text{(11e)}
\end{aligned}$$

where $[S] = \sum_k [S_k]$. The approximation in Eq. (10) is used to compute the pairs $[S_kI]$ and $[I_kS]$ for $k = 0, 1, \ldots, N-1$, and according to [9], the triples are closed by

$$[ASI] = \frac{[AS][SI]}{([SS]+[SI])^2}\sum_k k(k-1)[S_k].$$

Preliminary numerical investigations reveal that this compact model produces better qualitative agreement with results from simulation than the standard pairwise model. And although this agreement is not optimal, the model offers further value through providing qualitative insights into the behaviour of the degree distribution in time or

at equilibrium. A detailed study of the compact pairwise model is beyond the scope of the present paper, but below we present some output from this model with special focus on elucidating the types of networks that are likely to emerge.

We start by reporting on the behaviour of networks when the endemic steady state is stable. In Fig. 5 the degree distributions (shown as a non-normalised degree histogram here and in all subsequent figures) of the whole network and those of susceptible and infected nodes separately are plotted. This reveals that the emerging networks can vary both in their degree distribution and average degree. The most striking difference is the propensity of the infected nodes to become isolated compared to susceptible nodes. This effect is exacerbated in the left panel of Fig. 5. On the one hand, the network dynamics removes $S-I$ links thus reducing the number of edges originating from infected nodes. On the other hand, the network is replenished with $S-S$ links and these nodes enjoy and share more links compared to infected ones. In the true network-based stochastic simulation model this effect, for the right parameter combinations, can lead to complete isolation of the infected nodes through being cut off from the rest of the network, leading to the whole process being eventually attracted to the absorbing state with no infected nodes and all possible links present.

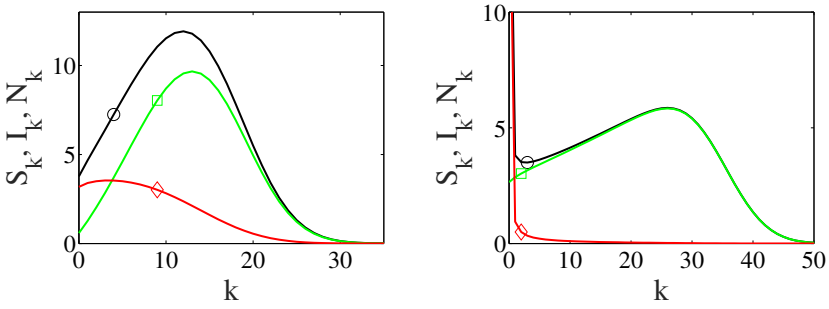

Fig. 5: Degree distributions (shown as a non-normalised degree histogram here and in all subsequent figures) of the susceptible (□), infected (◇), and the whole network (○) at the endemic steady state using the compact pairwise model (11). The parameter values are $N=200$, $\gamma=1$, and $\alpha_{SS}=0.04$ with (left-panel) $\tau=0.2$ and $\omega_{SI}=1.5$, and (right-panel) $\tau=4$ and $\omega_{SI}=100$.

Let us now focus on the oscillatory regime within the Hopf island. In the top panel of Fig. 6 we show a typical plot of the time evolution of both prevalence and average degree. We note that these oscillations go hand in hand but are out of phase. At high average degree the prevalence is typically small meaning that the network has many susceptible nodes that become more and more densely connected. However, as soon as infection manages to invade from the fringe of this tightly connected cluster of susceptible nodes, the epidemic spreads and the prevalence grows. As the number of infected nodes increases so does that of the $S-I$ links.

The link removal becomes significant and slows the epidemic due to fewer links being available for transmission.

The middle panel of Fig. 6 shows the typical degree distribution at the peak and trough of the degree oscillation. Again, as explained above, we notice that at the trough, when the average degree attains its minimum, the number of nodes with no or few connections increases significantly. As shown in the bottom two panels of the same figure, it is mainly the infected nodes that suffer the consequences of the link cutting process and these nodes lose many of their links leaving them with no or very few connections. In contrast, the susceptible nodes are more resilient and their degree distribution shows less dramatic change between peak and trough.

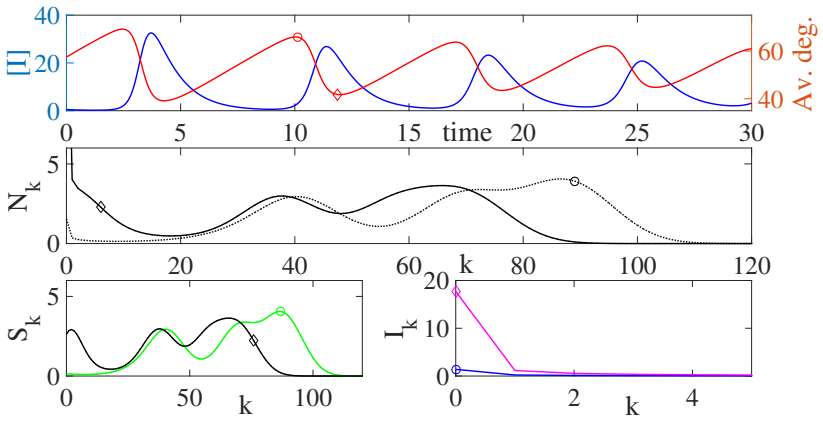

Fig. 6: Illustration of the oscillatory behaviour in the expected prevalence and average degree (the curve with the markers) based on the compact pairwise model (11) (top panel). Prevalence and average degree are out of phase with the network being most densely connected when the prevalence of infection is low and vice-versa. The degree distribution at the peak ($\circ$) and trough ($\diamond$) of the oscillatory cycle of the average degree (middle panel) shows that the network loses links and more poorly connected nodes emerge with the entire degree distribution moving towards lower degrees. The degree distribution of susceptible and infected nodes (bottom panel) reveal that infected nodes are in general poorly connected due to the cutting of $S-I$ links. Parameter values are: $N = 200$, $\tau = 0.4$, $\gamma = 1$, $\alpha_{SS} = 0.04$ and $\omega_{SI} = 25$. We note that the oscillations eventually stabilise with a well defined amplitude and cycle duration.

Analysing emerging networks using simulation

Finally, we present some results from rigorous network-based stochastic simulations using the Gillespie algorithm. Before we turn to the analysis of the output we recall some of the nuances of the comparison between mean-field and simulation models. First, it is well known that the worst performance of the mean-field models is usually when the system operates close to threshold, i.e., at the point separating die-out from an epidemic. Moreover, during oscillations that come close to extinction (i.e., a system with a small number of infected nodes), agreement with the mean-field models is also expected to break down. Typically in such cases, the stochastic process can be absorbed by the all-susceptible state, while the mean-field models will indicate oscillations.

In what follows we focus on the oscillatory regime and map out how both system and network behave during one cycle of oscillation. First, we note that the de-phasing between prevalence and average degree is not as clear as for the deterministic model, see Fig. 7. However, the trend is similar in that the average degree peaks before the epidemic peaks. Our analysis here is based on peaks and troughs in prevalence rather than average degree, as per the mean-field case. This is purely because oscillations in prevalence had a bigger amplitude and thus were easier to capture. However, we shall show this complements the results thus far. We also note that the parameter values for the simulation were chosen based on a simulation-based bifurcation diagram in [24]. This was necessary because the agreement between bifurcation boundaries in the mean-field and simulation models is qualitative rather than quantitative.

There is an interesting contrast between the four competing processes: (a) link creation, (b) link deletion, (c) transmission, and (d) recovery. These processes compete and balance out in order to give rise to oscillatory behaviour both in the prevalence and degree. This is illustrated in Fig. 7 where we also show a few explicit network snapshots during the main phases of a full cycle, including the trough and peak of the oscillation in prevalence. The main phases of the oscillation cycle are:

1. **Phase A:** $[I]$ decreasing, $\langle k \rangle$ decreasing with recovery and link cutting dominating transmission and link creation, respectively;
2. **Phase B:** $[I]$ decreasing, $\langle k \rangle$ increasing with recovery dominating transmission but link creation dominating link cutting;
3. **Phase C:** $[I]$ increasing, $\langle k \rangle$ increasing with transmission and link creation dominating recovery and link cutting, respectively;
4. **Phase D:** $[I]$ increasing, $\langle k \rangle$ decreasing with transmission dominating recovery but link cutting dominating link creation.

Several important observations can be made. The simulation captures different phases of the cycle. At peak prevalence the cutting of $S-I$ links has the biggest impact on the remaining few susceptible nodes. These become disconnected from the cluster of tightly connected infected nodes. Here, the S nodes are poorly connected while the I nodes share many links with other I nodes; see Fig. 7 and the corresponding degree distributions in Fig. 8. However, when the prevalence is low,

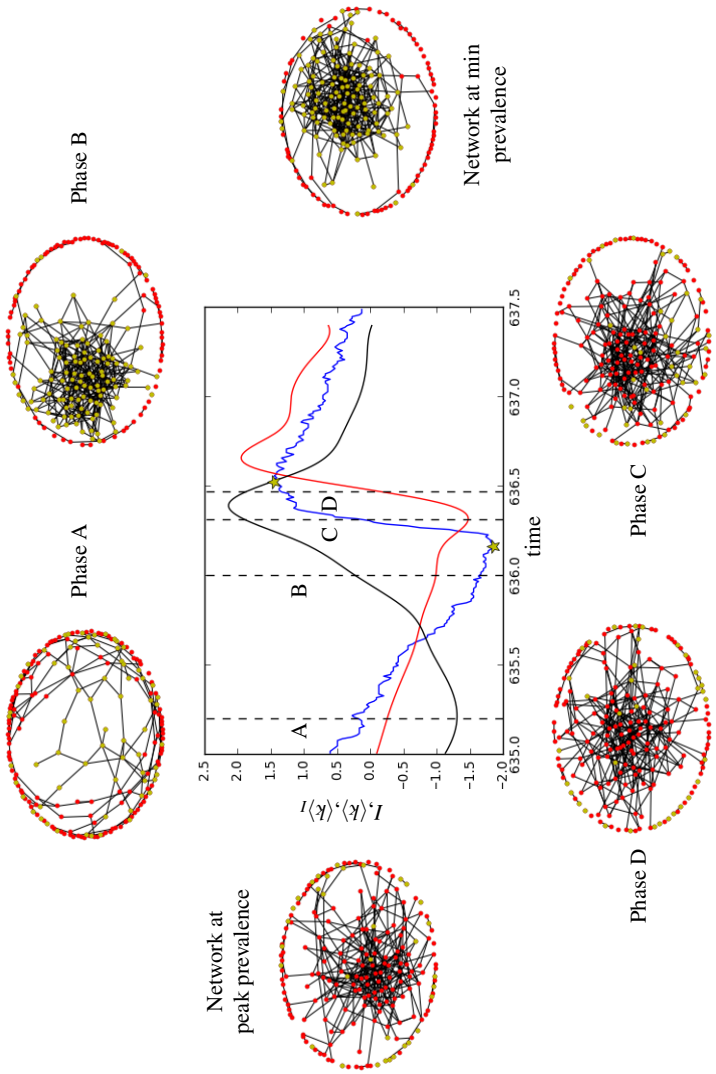

Fig. 7: A full cycle of oscillation of prevalence (blue, I), average degree of the whole network (black, $\langle k \rangle$) and of infected nodes (red, $\langle k \rangle_I$) based on a single realisation of the stochastic simulation (printed in portrait mode for clarity). All data series have been normalised as $\frac{X-\nu}{\sigma}$, where ν and σ are the mean and standard deviation of the data series taken over the time interval shown in the figure. The dashed lines denote the time points when the networks have been plotted and, more importantly correspond to the four Phases A, B, C and D of the oscillation cycle. The peak and trough of prevalence are highlighted by star symbols and the networks corresponding to these turning points are given at the bottom and top, respectively. Parameter values are $N = 200$, $\gamma = 1$, $\alpha_{SS} = 0.04$, $\tau = 6$ and $\omega_{SI} = 4$.

the infected nodes become isolated and the network is dominated by the cluster of susceptible nodes. Table 1 shows clearly that the average degree of infected nodes is small when the prevalence is at its trough, while the average degree of susceptible nodes attains its minimum when prevalence peaks.

Focusing on the case when prevalence is small, it is evident from Fig. 7 that the creation of $S-S$ links floods the subset of S nodes, making this part of the network well connected. At this point, the very few infected nodes that may still share links with the susceptible cluster can trigger a sizeable increase in infection prevalence. Of course, at this critical point, the epidemic may die out with some non-negligible probability if enough I nodes are isolated from the susceptible cluster.

To complement the heuristic network plots, the degree distributions of networks at Phases A, B, C and D are shown in Fig. 8. In contrast to the analysis based on the compact pairwise models, the simulation shows that the role reversal between the degree of S and I nodes, when going from peak to minimum prevalence, is more balanced and the number of poorly connected S and I nodes is comparable between Phases B and D. This of course may be parameter-specific and these regimes may be present in both models.

Looking at Tables 1 and 2 we note that the network undergoes significant changes and these are summarised below. The average degree achieves its highest value when the prevalence is at its minimum. The networks are sparsest in Phase A, when following a major increase in the prevalence level the network is thinned, and both the cutting of links and recovery dominate. Overall the observed networks remain fairly sparse and, as expected, the level of clustering is low. Table 2 shows the unique counts of a few chosen subgraphs for all six networks. Again, as expected, subgraphs are more numerous at the time point when prevalence is at its minimum.

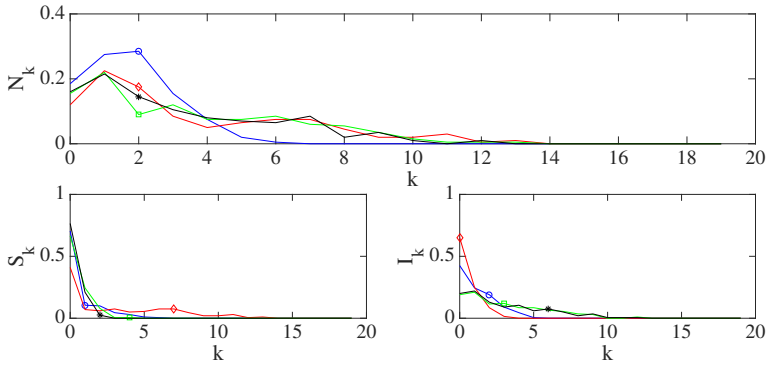

Fig. 8: Degree distributions of networks in Phase A (○), B (◇), C (□) and D (∗). In the top panel the degree distribution of the entire network is plotted independently of the status of the nodes. The bottom left and right panels focus on the degree distributions of susceptible and infected nodes, respectively. Parameter values are: $N = 200$, $\tau = 6$, $\gamma = 1$, $\alpha_{SS} = 0.04$ and $\omega_{SI} = 4$.

	Entire network						Giant component						
	[I]	[S]	n	n_I	n_S	C	[N]	[I]	[S]	n	n_I	n_S	C
A	132	68	1.74	1.67	1.88	0.02	134	84	50	2.28	2.15	2.50	0.02
B	83	117	3.59	1.12	5.34	0.08	128	18	110	5.11	1.72	5.66	0.08
Min	77	123	4.22	1.09	6.18	0.07	137	17	120	5.77	1.88	6.32	0.07
C	158	42	3.45	3.81	2.10	0.05	144	117	27	4.60	4.93	3.15	0.05
D	164	36	3.17	3.55	1.44	0.05	143	125	18	4.24	4.46	2.67	0.05
Max	166	34	3.13	3.51	1.26	0.05	142	127	15	4.20	4.40	2.47	0.05

Table 1: Summary network characteristics for the 6 networks considered in Fig. 7. Given the large number of components in the network, the table provides information both for the entire network and the giant component. The global clustering coefficient denoted by C in the Table was calculated using the formula proposed in [10]. The number of components (not shown) is fairly constant across networks (average of 43, min=37 at min prevalence, max=47 in network A). Network A has the largest number of nodes with degree 0 (37) and degree 1 (55). The network at min prevalence has the smallest number of nodes with degree 0 (21) and degree 1 (43).

	⊠	◪	□	△	⬠	⬡
A	0	0	5	2	6	3
B	3	37	143	9	544	2056
Min	3	51	289	7	1143	4558
C	0	8	117	14	331	1156
D	0	7	101	11	256	803
Max	0	6	95	12	230	771

Table 2: Number of uniquely counted subgraphs for each network as calculated by the subgraph counting algorithm described in [18]. It should be noted that the number of △ corresponds to △ not involved in either ⊠ or ◪.

4.3 Towards a bifurcation theory of dynamic networks

In formulating this problem, we restrict ourselves to undirected, unweighted networks with N nodes, where links are binary (i.e., either present or not). In this case the state space of all such networks $\mathscr{G}$ has cardinality $2^{N(N-1)/2}$. The body of work concerning the properties and the dynamics of and on such networks indicates that certain sub-sets of the whole state space are more likely to arise in applications and in theoretical work. Hence, considering subsets $\mathscr{G}_i \in \mathscr{G}$, where $\mathscr{G}_i$ correspond to classes of well-known networks (e.g., Erdős-Rényi random, lattice-type, clustered, scale-free etc) is a widely used approach.

This setup is particularly useful when considering dynamical processes evolving on a fixed network specified on the basis of empirical observations or a network model. However, when considering adaptive or evolving networks, i.e., when the dynamics on the network and that of the network are coupled, this approach needs to be made more rigorous. Let us first assume that we have a dynamics on the network where nodes can achieve a discrete number of possible states (i.e., $a_1, a_2, \ldots, a_m$) with transition rules and rates stored in an operator $\mathscr{D}$ (dynamic on the network). This operator is in fact of the form $\mathscr{D} = (D_{i,j})_{i,j=1,2,\ldots,m}$, where $D_{ij} = D_{ij}(r_{ij}, \mathscr{G})$ with r_{ij} describing the transition rate of a node in state a_j to state a_i, where this transition may or may not involve knowledge about the network (i.e., $\mathscr{G}$ - the network's adjacency matrix).

Another operator $\mathscr{H}$ specifies the dynamics of the network which may be vertex type-dependent (e.g., link activation and cutting, nodes birth and death and instant partner exchange). For link activation and deletion alone, this operator can be written as

$$\mathscr{H} = (H_{i,j})_{i=1,2,\ldots M, j=1,2},$$

where $M = m(m+1)/2$, $H_{i,1} = H_{i,1}(\alpha_{se(i)}, \mathscr{G})$ and $H_{i,2} = H_{i,2}(\omega_{se(i)}, \mathscr{G})$, where $se(i)$ is the ith element of the set describing all potential edge statuses

$$SE = \{a_1a_1, a_1a_2, \ldots a_1a_m, a_2a_2, a_2a_3, \ldots, a_2a_m, a_3a_3, \ldots, a_ma_m\}.$$

If, for example, instant partner switching is to be implemented, $\mathscr{H}$ can be augmented by $\mathscr{L} = (L_{ij})_{i,j=1,2,\ldots,m^2}$, where L_{ij} is simply the rate at which edges of type $se(j)$ switch to edges of type $se(i)$. Particular interest is paid to understanding how the topology of the network changes under the action of different dynamics on and of the network and how these are coupled. This naturally leads to the question of how to translate the mathematical concepts and tools from the *bifurcation theory of dynamical systems* to a *bifurcation theory of dynamical networks*.

For example, in the case of a simple epidemic model such as *SIS* (susceptible-infected/infectious-susceptible, where τ is the per-contact infection rate and γ is the recovery rate), coupled with the activation and deletion of links of different statuses (i.e., $SE = \{SS, SI, II\}$) and with partner switching or smart rewiring, where the S node in an $S-I$ rewires to a randomly chosen other susceptible, the entire dynamics can be captured by the following operators,

$$\mathscr{D} = \begin{pmatrix} 0 & \gamma \\ \tau = \tau_G & 0 \end{pmatrix}, \quad \mathscr{H} = \begin{pmatrix} \alpha_{SS} & \omega_{SS} \\ \alpha_{SI} & \omega_{SI} \\ \alpha_{II} & \omega_{II} \end{pmatrix} \text{ and } \mathscr{L} = \begin{array}{c} \\ SS \\ SI \\ IS \\ II \end{array} \begin{array}{c} \begin{array}{cccc} SS & SI & IS & II \end{array} \\ \begin{pmatrix} 0 & \omega & 0 & 0 \\ 0 & 0 & 0 & 0 \\ 0 & 0 & 0 & 0 \\ 0 & 0 & 0 & 0 \end{pmatrix} \end{array}.$$

In this relatively well-studied case [7, 12, 24] and given the results in this chapter, the following observations can be made:

1. if link activation and deletion are link status-independent (i.e., Scenario A and $\omega = 0$ in $\mathscr{L}$), then at equilibrium the resulting network will be an Erdős-Rényi random network;
2. if link activation and deletion are link status-independent (i.e., Scenario A and $\omega = 0$ in $\mathscr{L}$) then at the critical cutting rate α^*, see equation (7) and Fig. 2, the network will transition from being connected to disconnected, or vice-versa;
3. in Scenario B (and $\omega = 0$ in $\mathscr{L}$) and at the endemic equilibrium, depending on the precise parameter values, the network at equilibrium may or may not have a high density of poorly connected nodes, see Fig. 5;
4. in [7], for smart rewiring, it was shown that when $\mathscr{H} = 0$ then depending on the rewiring or partner switching rate ω the network transitions from being connected to disconnected, or vice-versa.

The interplay between $\mathscr{D}$, $\mathscr{H}$ and $\mathscr{L}$ leads to a *bifurcation in the network topology*, where under the action and interaction of dynamical processes, the network can evolve towards different topologies/structures. This type of parameter-dependent change or evolution in network structure is analogous to bifurcations in dynamical systems, and we can interpret the change in network topology as certain network steady states losing or gaining stability at the cost of other network steady states gaining or losing stability.

As seen in the results section above, there is a subtlety as to what can be regarded as a significant enough difference between two networks in order to be classified as a different behaviour type. For example using the simple pairwise model we have seen that the average degree can vary significantly, see Fig. 4, but this may not be regarded as a sufficiently different outcome. In general, we believe that the partitioning of the graph state space $\mathscr{G}$ in terms of known network types may not be the ideal resolution. Nevertheless, we conjecture that it will be possible to give results such as the one below.

Conjecture: *Given a spreading process defined by $\mathscr{D}$, and a dynamic network given by $\mathscr{H}$ and $\mathscr{L}$, with the respective set of transition rates, $\mathscr{T}\mathscr{R} \in \mathbb{R}^d$ (d - total number of parameters), one can determine a mapping $\mathscr{M} : \mathbb{R}^d \to \cup_i \mathscr{G}_i$ which identifies the bifurcation manifolds, whereby given a fixed set of parameters, the asymptotic behaviour (e.g., steady-state, quasi steady state and limit cycle) of the network structure can be specified.*

5 Discussion

In this chapter we set out to redress the balance between analysis at system level and analysis of the emerging network structures by focusing on the latter. Starting from the simplest pairwise model and guided by its bifurcation analysis we showed that when the epidemic is at the endemic equilibrium, the average degree of the network attains a wide range of values and bistable-like behaviour is observed, where the same average degree is achieved at the same value of the transmission rate, τ, but different cutting rates, ω.

Recognising the importance of the degree distribution as defining a network, we moved to the compact pairwise model which apart from the status of the nodes also tracks their degree. This model allowed us to show that the emerging networks can be significantly different at the peak and trough of the oscillations, and that at equilibrium and depending on the parameter values, networks with significantly different degree distributions emerge. The analysis of the stochastic model via simulation revealed a range of networks during the oscillatory cycle and highlighted a role reversal between susceptible and infected nodes when going from high to low prevalence. We also speculated mathematically about the shape a bifurcation theory for networks may take.

Several important questions remain. First of all, the bifurcation analysis of the compact pairwise model needs to be completed as this may reveal additional features or richer model behaviour. This may be challenging as the system is high-dimensional so the analysis may be restricted to numerical investigations alone. A big open question remains about the validity of such mean-field models for systems where dynamic on and of the network are coupled. As explained above, this may lead to networks becoming disconnected as well as excessive correlations between nodes of different status, all being factors that may invalidate mean-field models. Nevertheless, there is some evidence that mean-field models still play an important role in getting an initial insight into analysing such models.

The numerical investigation of the phases of the oscillatory cycle needs to be extended to include many different parameter values and assess how the resulting networks change. In addition, a similar type of numerical investigation or simulation should be carried out when the epidemic stabilises to the endemic state. Perhaps more importantly, different dynamics should be considered which may lead to even richer network-level behaviour. Such dynamics may include voter model, complex contagion, neuronal dynamics with homeostatic plasticity.

Mathematically, the problem of characterising the emerging network structure in a bifurcation theory-like fashion may prove to be challenging, partly due to the mean-field systems being high-dimensional. Overlooking the problem of whether mean-field models agree well with the average behaviour of the exact stochastic process, the analysis of such mean-field models may be best considered like a discretisation of a partial differential equation, thus allowing us to derive a more compact model which is amenable to analysis. Examples of this type can be found in [21].

Finally, given that it is reasonable to expect that many real-world networks are in fact time-frozen snapshots of an otherwise evolving system, we argue that such a network-focused view is not only desirable but could stimulate the development or design of more natural network-generating algorithms with stronger direct links to realistic processes.

Acknowledgements Joel C. Miller was funded by the Global Good Fund through the Institute for Disease Modeling and by a Larkins Fellowship from Monash University. Péter L. Simon acknowledges support from Hungarian Scientific Research Fund, OTKA, (grant no. 115926).

References

1. Ball, F., Neal, P.: Network epidemic models with two levels of mixing. Mathematical Biology **212**(1), 69–87 (2008)
2. Chung, F.R., Lu, L.: Complex graphs and networks, vol. 107. American Mathematical Society Providence (2006)
3. Danon, L., Ford, A.P., House, T., Jewell, C.P., Keeling, M.J., Roberts, G.O., Ross, J.V., Vernon, M.C.: Networks and the epidemiology of infectious disease. Interdisciplinary Perspectives on Infectious Diseases **2011** (2011)
4. Durrett, R.: Random Graph Dynamics. Cambridge U. Press (2007)
5. Eames, K., Keeling, M.: Modeling dynamic and network heterogeneities in the spread of sexually transmitted diseases. Proc. Natl. Acad. Sci. USA **99**(20), 13,330–13,335 (2002)
6. Gross, T., Blasius, B.: Adaptive coevolutionary networks: a review. Journal of the Royal Society Interface **5**(20), 259–271 (2008)
7. Gross, T., D'Lima, C.J.D., Blasius, B.: Epidemic dynamics on an adaptive network. Physical Review Letters **96**(20), 208,701 (2006)
8. Gross, T., Kevrekidis, I.G.: Robust oscillations in sis epidemics on adaptive networks: Coarse graining by automated moment closure. Europhysics Letters **82**(3), 38,004 (2008)
9. House, T., Keeling, M.: Insights from unifying modern approximations to infections on networks. Journal of the Royal Society Interface **8**(54), 67–73 (2011)
10. Keeling, M.J.: The effects of local spatial structure on epidemiological invasions. Proceedings of the Royal Society B: Biological Sciences **266**(1421), 859–867 (1999)
11. Kiss, I., Miller, J., Simon, P.: Mathematics of Epidemics on Networks: from Exact to Approximate Models. IAM. Springer (2017)
12. Kiss, I.Z., Berthouze, L., Taylor, T.J., Simon, P.L.: Modelling approaches for simple dynamic networks and applications to disease transmission models. Proc. R. Soc. A **468**(2141), 1332–1355 (2012)
13. Lindquist, J., Ma, J., van den Driessche, P., Willeboordse, F.: Effective degree network disease models. Journal of Mathematical Biology **62**(2), 143–164 (2011). DOI 10.1007/s00285-010-0331-2
14. Marceau, V., Noël, P.A., Hébert-Dufresne, L., Allard, A., Dubé, L.J.: Adaptive networks: Coevolution of disease and topology. Physical Review E **82**(3), 036,116 (2010)
15. Miller, J.C., Kiss, I.Z.: Epidemic spread in networks: existing methods and current challenges. Mathematical Modelling of Natural Phenomena **9**(02), 4–42 (2014)
16. Miller, J.C., Slim, A.C., Volz, E.M.: Edge-based compartmental modelling for infectious disease spread. Journal of the Royal Society Interface **9**(70), 890–906 (2012). DOI 10.1098/rsif.2011.0403
17. Pastor-Satorras, R., Castellano, C., Van Mieghem, P., Vespignani, A.: Epidemic processes in complex networks. Reviews of Modern Physics **87**(3), 925–979 (2015)
18. Ritchie, M., Berthouze, L., House, T., Kiss, I.Z.: Higher-order structure and epidemic dynamics in clustered networks. Journal of Theoretical Biology **348**, 21–32 (2014)
19. Rogers, T., Clifford-Brown, W., Mills, C., Galla, T.: Stochastic oscillations of adaptive networks: application to epidemic modelling. Journal of Statistical Mechanics: Theory and Experiment **2012**(08), P08,018 (2012)
20. Sayama, H., Pestov, I., Schmidt, J., Bush, B.J., Wong, C., Yamanoi, J., Gross, T.: Modeling complex systems with adaptive networks. Computers & Mathematics with Applications **65**(10), 1645–1664 (2013)
21. Silk, H., Demirel, G., Homer, M., Gross, T.: Exploring the adaptive voter model dynamics with a mathematical triple jump. New Journal of Physics **16**(9), 093,051 (2014)
22. Szabó, A., Simon, P.L., Kiss, I.Z.: Detailed study of bifurcations in an epidemic model on a dynamic network. Differ. Equ. Appl **4**, 277–296 (2012)
23. Szabó-Solticzky, A.: Dynamics of a link-type independent adaptive epidemic model. Differ. Equ. Appl. (Accepted)

24. Szabó-Solticzky, A., Berthouze, L., Kiss, I.Z., Simon, P.L.: Oscillating epidemics in a dynamic network model: stochastic and mean-field analysis. Journal of Mathematical Biology **72**(5), 1153–1176 (2016)
25. Taylor, M., Taylor, T.J., Kiss, I.Z.: Epidemic threshold and control in a dynamic network. Physical Review E **85**(1), 016,103 (2012)